

One-pot synthesis of $\text{VO}_x/\text{Al}_2\text{O}_3$ as efficient catalysts for propane dehydrogenation

Guangjian WANG* , Hao XU , Kai LU , Zhihao DING , Liancheng BING 
School of Chemical Engineering, Qingdao University of Science and Technology, Qingdao, P.R. China

Received: 25.07.2019

Accepted/Published Online: 30.10.2019

Final Version: 11.02.2020

Abstract: Vanadium oxides, as highly efficient catalysts, are widely applied in various catalytic reactions, such as the dehydrogenation of light alkanes and epoxidation of alkenes. In this paper, a series of $\text{VO}_x/\text{Al}_2\text{O}_3$ catalysts were fabricated by the 1-pot method for catalytic propane dehydrogenation. The results indicated that the $\text{VO}_x/\text{Al}_2\text{O}_3$ catalysts with loading of 10 wt.% vanadium exhibited optimized catalytic performance. The as-prepared catalysts were characterized by N_2 adsorption-desorption, XRD, TEM, H_2 -TPR, and XPS to explore the texture properties, morphology, and electronic environment of vanadium. In addition, several vanadium catalysts were also prepared by the incipient wetness impregnation (IWI) method to compare their catalytic performance with the 1-pot synthesized catalysts. The catalysts synthesized by the 1-pot method exhibited higher selectivity of propylene and longer catalyst lifetime at high propane conversion when compared to the counterpart synthesized by the IWI method.

Key words: One-pot synthesis, propane dehydrogenation, $\text{VO}_x/\text{Al}_2\text{O}_3$ catalysts

1. Introduction

Propylene is a fundamental and key feedstock for the production of important chemical intermediates such as polypropylene, acrylonitrile, and 2-propanol [1]. The production of propylene from catalytic propane dehydrogenation (PDH) using platinum (Pt)- or chromium oxide (CrO_x)-based catalysts is practiced commercially, but the restructuring of Pt and CrO_x species is also a great challenge for the stability of catalysts after regeneration [2–4]. Moreover, Pt- or CrO_x -based catalysts are limited because Pt-based catalysts employ noble metal, while CrO_x -based catalysts create pollution of the environment [5,6]. Vanadium, as a cost-effective and environmentally friendly metal, is an attractive alternative catalyst for PDH [7]. Although vanadium catalysts are mainly applied in the oxidative dehydrogenation of propane, researchers have found that they also displayed excellent catalytic performance and high stability for PDH [8,9]. For instance, Gong et al. found that $\text{VO}_x/\text{Al}_2\text{O}_3$ catalysts prepared by the incipient wetness impregnation (IWI) method exhibited extremely high selectivity for propylene (80%) with 35% conversion of propane [5]. The surface-bound hydroxyl groups on $\text{VO}_x/\text{Al}_2\text{O}_3$ played an important role in catalytic performance for PDH. Ovsitser et al. reported the synthesis of $\text{VO}_x/\text{Al}_2\text{O}_3$ by the IWI method for PDH with 80% propylene selectivity and 45% propane conversion [10]. Sokolov et al. found that VO_x -supported MCM-41 exhibited high stability for PDH, being more stable than Pt/MCM-41 or $\text{CrO}_x/\text{MCM-41}$ catalysts [11]. Yan et al. found that the crystalline temperature of aluminum had great influence on the catalytic performance of $\text{VO}_x/\text{Al}_2\text{O}_3$ catalysts, and catalysts with loading of 10

*Correspondence: shiyanshi304@163.com

wt.% vanadium displayed high propane conversion and propylene selectivity [12]. Despite the enhancement of catalytic performance, these catalysts, prepared by the multistep synthetic method, normally result in the poor dispersion of active metal [13].

It is worth noting that the superior catalytic performances of 1-pot synthesized metal catalysts were proved via numerous related studies due to the good dispersion and sintering resistance of active metals [14,15]. The dispersion of active metal and strong metal-support interaction dramatically enhanced the catalytic efficiency of catalysts [16]. Significant progress has been made in metal or metal oxide catalysts synthesized by the 1-pot method with the incorporation of various metals, including Pt, Pb, Ni, and Mo [17–20]. For instance, Guo et al. used VO_x/SiO_2 catalysts synthesized by the 1-pot method to obtain a high propane conversion of 45% [21]. Chu and Luo reported PtSn/Mg-SBA-15 catalysts that achieved high catalytic performance for PDH [22]. Filez et al. synthesized Pt-based catalysts by the 1-pot method that achieved superior catalytic performance for PDH [23]. To date, however, there have been no reports on the synthesis of $\text{VO}_x/\text{Al}_2\text{O}_3$ catalysts via the 1-pot method.

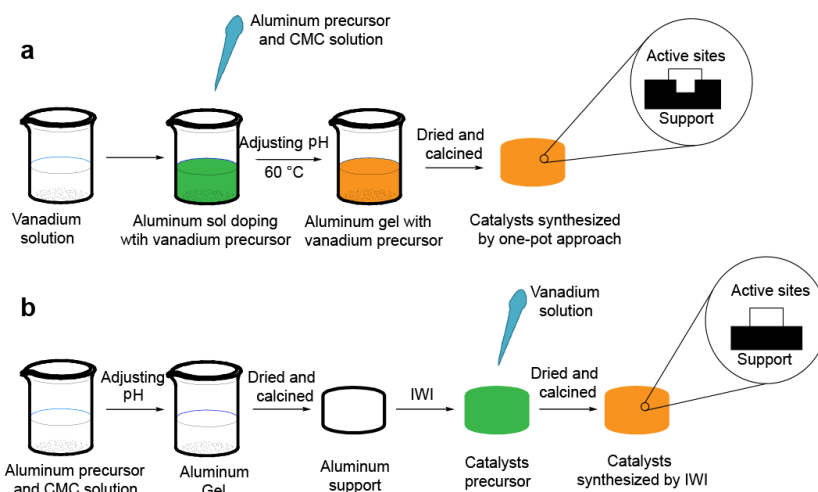
In this paper, we present a facile 1-pot method to synthesize $\text{VO}_x/\text{Al}_2\text{O}_3$ catalysts, which are highly efficient, cost-effective, and environmentally friendly. Unlike other $\text{VO}_x/\text{Al}_2\text{O}_3$ catalysts prepared by the multistep synthetic method, good dispersion of the active metal (VO_x) can be obtained during the formation of catalysts. The $\text{VO}_x/\text{Al}_2\text{O}_3$ catalysts were synthesized through the 1-pot method combined with evaporation-induced self-assembly (EISA) using sodium carboxymethyl cellulose (CMC) as an anionic surfactant [24–26]. As can be seen in the Scheme, the introduction of vanadium species was achieved by adding the solution of aluminum nitrate and CMC into the solution of the vanadium precursor. Next, aqueous ammonia was added to enhance the assembly by promoting the interaction between the vanadium precursor and CMC. Moreover, aluminum oligomer, derived from aluminum nitrate during hydrolysis, can interact with the CMC by hydrogen bonding, ensuring assembly with the vanadium precursor. In short, the alumina and vanadium oxide precursors were mixed in solution state and CMC was used as an anionic surfactant. The vanadium precursor dispersed uniformly in the framework of alumina gel during the evaporation self-assembly process and eventually formed a vanadium-doping disordered Al_2O_3 catalyst. Meanwhile, a series of $\text{VO}_x/\text{Al}_2\text{O}_3$ catalysts were also synthesized by the IWI method to compare the catalytic performance with that of the $\text{VO}_x/\text{Al}_2\text{O}_3$ catalysts synthesized by the 1-pot method. It was found that the catalysts prepared by the 1-pot method exhibited higher catalytic performance and stability than those prepared by the IWI method, and the O-10- $\text{VO}_x/\text{Al}_2\text{O}_3$ catalysts displayed optimized catalytic performance. In addition, properties of the catalysts were investigated by N_2 adsorption-desorption, XRD, TEM, H_2 -TPR, and XPS for a better understanding of catalytic behavior.

2. Experimental

2.1. Catalyst synthesis

2.1.1. One-pot method

One-pot synthesized $\text{VO}_x/\text{Al}_2\text{O}_3$ catalysts, with loading of 10 wt.% vanadium, were prepared via the 1-pot method combined with EISA. A specific amount of ammonium metavanadate and oxalic acid was dissolved at 60 °C using a beaker in 160 mL of deionized water to form a clear solution. The molar ratio of ammonium metavanadate and oxalic acid was 1:1. The solutions of aluminum nitrate and CMC were subsequently added to the solution of ammonium metavanadate under vigorous stirring. Aqueous ammonia was then dropped into the mixture until the pH value was modified to 8, followed by stirring at 60 °C for 8 h. At the end of stirring,



Scheme. One-pot (a) and IWI (b) methods for preparing the $\text{VO}_x/\text{Al}_2\text{O}_3$ catalysts.

the green precipitations were dried in an oven at $100\text{ }^\circ\text{C}$ for 12 h. Next, the precursors were calcined at $550\text{ }^\circ\text{C}$ for 10 h to obtain the O-10- $\text{VO}_x/\text{Al}_2\text{O}_3$ catalysts, where O represents the 1-pot synthesis. Other catalysts synthesized by the 1-pot method were prepared with different vanadium contents.

2.1.2. Incipient wetness impregnation method

In a typical process, a specific amount of ammonium metavanadate and oxalic acid was dissolved at $60\text{ }^\circ\text{C}$ using a beaker in 60 mL of deionized water to form a clear solution. The molar ratio of ammonium metavanadate and oxalic acid was 1:1.

To synthesize mesoporous aluminum, CMC was subsequently added to the solution of aluminum nitrate under vigorous stirring. The pH of the solution was then modified from 2 to 8 at $60\text{ }^\circ\text{C}$ under stirring to form uniform precipitates. The uniform precipitates were dried in an oven at $100\text{ }^\circ\text{C}$ for 12 h and then calcined in a muffle furnace at $550\text{ }^\circ\text{C}$ for 10 h, and the obtained mesoporous aluminum was used as supports.

The catalysts, with loading of 10 wt.% vanadium, were prepared by the IWI method. The mesoporous aluminum was impregnated with metavanadate solution and then dried at $100\text{ }^\circ\text{C}$ for 12 h. The catalysts were subsequently calcined at $550\text{ }^\circ\text{C}$ for 10 h. The resulting catalysts were denoted as I-10- $\text{VO}_x/\text{Al}_2\text{O}_3$, where I represents the incipient wetness impregnation method. Other impregnation catalysts were prepared with different vanadium contents.

2.2. Characterizations

N_2 adsorption-desorption isotherms of all of the samples were obtained with an Autosorb-1 (Quantachrome Instruments Inc., Boynton Beach, FL, USA). The surface areas and total pore volumes of the catalysts were obtained by the Brunauer–Emmett–Teller (BET) method and the N_2 adsorption amount was at a relative pressure of $P/P_0 = 0.99$. The size distribution curves of the mesopores and micropores were determined from the adsorption-desorption isotherms using the Barrett–Joyner–Halenda and Horvath–Kawazoe methods, respectively. X-ray powder diffraction (XRD) spectra were obtained with an X'Pert PRO MPD diffractometer (Malvern Panalytical Ltd., Malvern, UK) with $\text{Cu K}\alpha$ radiation ($\lambda = 0.1542\text{ nm}$). H_2 -TPR curves of the samples were collected on an Autosorb-iQ (Quantachrome Instruments) by a thermal conduction detector. Transmission electron microscopic (TEM) images were obtained using a JEM-2010 microscope (JEOL Ltd.,

Akishima, Tokyo, Japan) at an accelerating voltage of 200 kV. X-ray photoelectron spectroscopy (XPS) measurements were carried out by a Thermo Fisher ESCALAB 250 X-ray photoelectron spectrometer (Waltham, MA, USA) equipped with an Al K α X-ray source.

2.3. Catalytic performance

Catalytic reactions were performed in a continuous flow evaluation device, which included a mass flow controller, stainless steel reactor (10 nm), exhaust gas treatment unit, and analysis system. Under a N₂ flow of 30 mL/min, the stainless steel reactor loading samples of 3 g was heated from 20 °C to 550 °C within 3 h. Next, the N₂ flow was replaced by a H₂ flow of 5 mL/min to reduce the catalysts for 8 h at 550 °C. After that, the temperature was increased to 610 °C and the H₂ flow was closed. Next, a propane flow of 60 mL/min was introduced into the reactor, and the products were analyzed online by an Agilent 7820A GC (Santa Clara, CA, USA).

$$X (\%) = ([N_{C_3H_8}]_{in} - [N_{C_3H_8}]_{out}) / [N_{C_3H_8}]_{in}$$

$$Y (\%) = ([N_{C_3H_6}]_{out} - [N_{C_3H_6}]_{in}) / [N_{C_3H_8}]_{out}$$

$$S (\%) = ([N_{C_3H_6}]_{out} - [N_{C_3H_6}]_{in}) / ([N_{C_3H_8}]_{in} - [N_{C_3H_8}]_{out})$$

The above formulas were used to analyze the results of the experiment, where the conversion of propane and the yield and selectivity of propylene are represented by X, Y, and S, respectively. N_{C₃H₈} and N_{C₃H₆} are the number of carbon atoms, where C₃H₈ and C₃H₆ represent propane and propylene, respectively.

3. Results and discussion

3.1. Catalytic performance

Catalysts prepared by different methods were investigated to obtain the catalytic performance for PDH and the results are shown in Figure 1. It can be seen that the conversion of propane and yield of propylene increased rapidly during the initial 30 min for all of the catalysts and then decreased slowly after reaching the peak, which may have been due to the formation of carbon coating on the active sites [12]. At the same time, the selectivity of propylene was stable after a sharp drop. Among the 3 catalysts synthesized by the 1-pot method, the O-10-VO_x/Al₂O₃ catalysts showed the highest catalytic performance with an optimized propane conversion of 50% and propylene selectivity of 85% at 1 h of PDH reaction, while the O-8-VO_x/Al₂O₃ catalysts exhibited the poorest catalytic activity. For the O-10-VO_x/Al₂O₃ catalysts, the propane conversion and propylene selectivity fluctuated between 35% and 50% and between 84% and 89%, respectively. This may have been due to the deactivation of active sites caused by carbon deposition.

When compared with the VO_x/Al₂O₃ catalysts synthesized by the IWI method, the inactivation rate of those synthesized by the 1-pot method was slower, indicating that the catalysts synthesized by the 1-pot method had a longer catalytic lifetime than those synthesized by the IWI method [27]. In addition, after 4 h of reaction, the O-10-VO_x/Al₂O₃ catalysts still displayed the best catalytic activity, while the I-10-VO_x/Al₂O₃ catalysts had poor catalytic activity. This further demonstrated that the catalysts prepared by the 1-pot method had higher catalytic performance for PDH. Moreover, the turnover frequency (TOF) values of the as-prepared catalysts in PDH were calculated by $TOF_i = \frac{M_V X_i n_i^0}{m_{cat} c_V}$ to investigate the catalytic activity of the catalysts, where M_V, X_i, n_i⁰, m_{cat}, and c_V are the atomic mass of vanadium (50.94 g/mol), conversion of component i, molar flow rate of component i (mol/s), catalyst mass (g), and mass fraction of vanadium doping in the catalysts, respectively [2]. The results are shown in Table S1 and the O-10-VO_x/Al₂O₃ catalysts still exhibited the

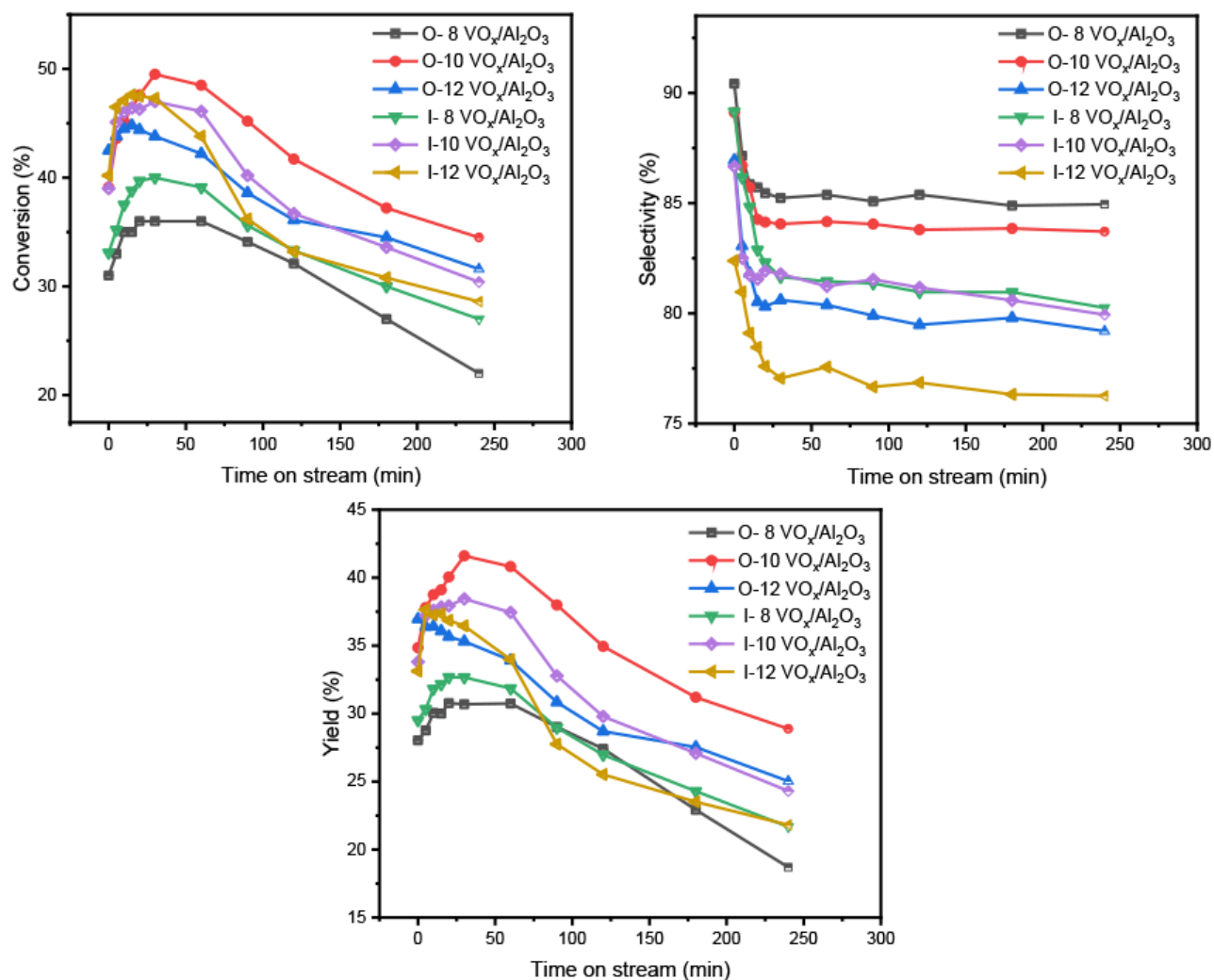


Figure 1. Catalytic performance of the vanadium catalysts prepared by one-pot method and IWI method.

highest catalytic activity. A summary of the catalytic data of the PDH catalysts is summarized in Table 1. When compared with the vanadium-based catalysts available in the recent literature, the propane conversion of the O-10-VO_x/Al₂O₃ catalysts synthesized herein was higher than that of the VO_x/Al₂O₃ catalysts prepared by the IWI method under similar reaction conditions, which was related to the high dispersion of vanadium and stable active sites. Although the propane conversion and propylene selectivity were similar to those of the VO_x/SiO₂ catalysts, the space velocity of the O-10-VO_x/Al₂O₃ catalysts was higher. When compared with Pt and CrO_x catalysts, the catalytic activity of the O-10-VO_x/Al₂O₃ catalysts for PDH was higher than that of the CrO_xNa/Al₂O₃ catalysts, which was similar to that of the Pt catalyst [28,29]. Moreover, the catalysts prepared herein were efficient, cost-effective, and environmentally friendly.

3.2. BET

N₂ adsorption-desorption was performed to analyze the detailed textural properties of the as-prepared catalysts. For the catalysts synthesized by the 1-pot method, catalysts with different vanadium doping presented similar N₂

Table 1. Summary of the catalytic data of the dehydrogenation catalysts.

| Catalysts | Active metal | Temperature | Propane conversion (2 h) | Propylene selectivity (2 h) | WHSV (h^{-1}) | Refs. |
|-----------------------------------------------|----------------|-------------|--------------------------|-----------------------------|--------------------------|-----------|
| $^a\text{VO}_x/\text{Al}_2\text{O}_3$ | VO_x | 610 °C | 42% | 85% | 1.2 | This work |
| VO_x/SiO_2 | VO_x | 580 °C | 45% | 90% | 0.3 | 2 |
| $\text{VO}_x/\text{Al}_2\text{O}_3$ | VO_x | 600 °C | 25% | 79% | 8 | 5 |
| $\text{VO}_x/\text{MCM-41}$ | VO_x | 600 °C | 45% | 80% | 0.48 | 11 |
| $\text{CrO}_x\text{Na}/\text{Al}_2\text{O}_3$ | CrO_x | 550 °C | 42% | 80% | 0.12 | 29 |
| $\text{Pt-Sn}/\text{Al}_2\text{O}_3$ | Pt | 590 °C | 45% | 96% | 5.2 | 28 |

adsorption-desorption isotherms (Figure 2), which were type-IV isotherms with H-2 hysteresis loops according to the IUPAC classification, implying that they had an ink-bottle mesoporous structure. Meanwhile, the catalysts synthesized by the IWI method exhibited a type-IV isotherm with H-1 hysteresis loops, suggesting that the synthetic method could influence the mesoporous structure of $\gamma\text{-Al}_2\text{O}_3$. As can be seen in Table 2, the catalysts synthesized by the 1-pot method had a higher specific surface area and pore volume, which may have been due to the interaction between the vanadium precursor as well as the change of the weak interaction between the alumina precursor and CMC [30]. Moreover, the larger specific surface area increased the access between propane and the active sites, leading to higher catalytic performance of the catalyst for PDH. In addition, increased vanadium doping led to a decrease in the specific surface area and pore size, indicating that the VO_x species were located in the channel of $\gamma\text{-Al}_2\text{O}_3$ [2]. Moreover, a decrease in the hysteresis loop length of the samples was observed with increasing vanadium incorporation, simultaneously accompanied by decreases in the pore volume, which indicated that the amount of vanadium doping could remarkably affect the texture properties of catalysts and correspondingly affect the catalytic performance of the catalyst. The O-10- $\text{VO}_x/\text{Al}_2\text{O}_3$ catalysts had a proper pore structure, specific surface area, and vanadium content, which resulted in optimized catalytic performance.

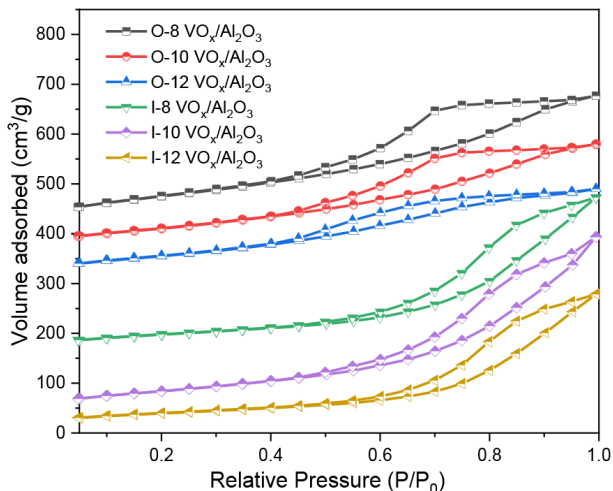
**Figure 2.** N_2 adsorption-desorption isotherms of the catalysts.

Table 2. Textural properties of the as-prepared catalysts.

| Catalysts | S_{BET} (m ² /g) | D_{BJH} (nm) | V_t (cm ³ /g) |
|------------------------------------------------------|-------------------------------|----------------|----------------------------|
| O-8-VO _x /Al ₂ O ₃ | 276 | 17.1 | 0.36 |
| O-10-VO _x /Al ₂ O ₃ | 224 | 18.1 | 0.31 |
| O-12-VO _x /Al ₂ O ₃ | 209 | 19.2 | 0.26 |
| I-8-VO _x /Al ₂ O ₃ | 198 | 18.1 | 0.30 |
| I-10-VO _x /Al ₂ O ₃ | 175 | 19.2 | 0.28 |
| I-12-VO _x /Al ₂ O ₃ | 162 | 20.1 | 0.23 |

3.3. XRD

The powder XRD patterns of the catalysts loaded with different vanadium contents are shown in Figure 3. For the catalysts synthesized by the 1-pot method, the broad peaks at 45.8° and 66.8° can be assigned to the structure of γ -Al₂O₃. There was no observable peak attributable to crystalline V₂O₅ for any of the catalysts with vanadium loading below 12 wt.%, which can be ascribed to high dispersion, and the size of the vanadium species was less than 2 nm. For the I-10-VO_x/Al₂O₃, no observable peak of VO_x was detected, indicating that there was no vanadium oxide on the catalysts prepared by the IWI method. Interestingly, the characteristic peak at 37.5° assigned to Al₂O₃ gradually decreased with increased vanadium incorporation. In contrast, the peak was significantly clearer in I-10-VO_x/Al₂O₃, despite having the same vanadium content as the O-10-VO_x/Al₂O₃ catalysts, which may have been due to the stronger interaction between the VO_x and supports.

3.4. TPR

To determine the reducibility and stability of the as-prepared catalysts, H₂-TPR measurements were performed. The TPR patterns of all of the catalysts between 300 and 720 °C are shown in Figure 4. The reduction peaks in the range of 490–510 °C of the catalysts prepared by the 1-pot method can be assigned to uniformly monomeric and/or low polymeric vanadium species, indicating that the active sites were anchored on the support stably [31–33]. When compared with the catalysts synthesized by the 1-pot method, the reduction peak of the catalysts synthesized by the IWI method slightly shifted to a high temperature, suggesting that the dispersion of vanadium on the catalyst prepared by the IWI method was worse. A shoulder peak at 560 °C was observed in the I-8-VO_x/Al₂O₃ catalysts, which may be attributed to the aggregation of vanadium species [2]. Meanwhile, additional reduction peaks at 634 °C in the I-10-VO_x/Al₂O₃ and I-12-VO_x/Al₂O₃ catalysts were observed, which may have been due to the presence of V₂O₅ crystallites [21]. By combining the BET and XRD analyses, it can be concluded that the catalysts prepared by the 1-pot method presented higher dispersion of vanadium and more stable active sites. Previous literature has shown that monomeric and/or low polymeric vanadium species are the main active species for PDH reaction [31]. Hence, the catalysts prepared by the 1-pot method exhibited higher catalytic performance and stability than those prepared by the IWI method for PDH.

3.5. TEM and XPS

To investigate the morphology of the catalysts and dispersion of the vanadium species, TEM characterization was performed for the O-10-VO_x/Al₂O₃ catalysts. Figures 5a and 5b display the TEM images of the O-10-VO_x/Al₂O₃ catalysts. The catalysts exhibited a disordered worm-like channel, in which the fine stripes

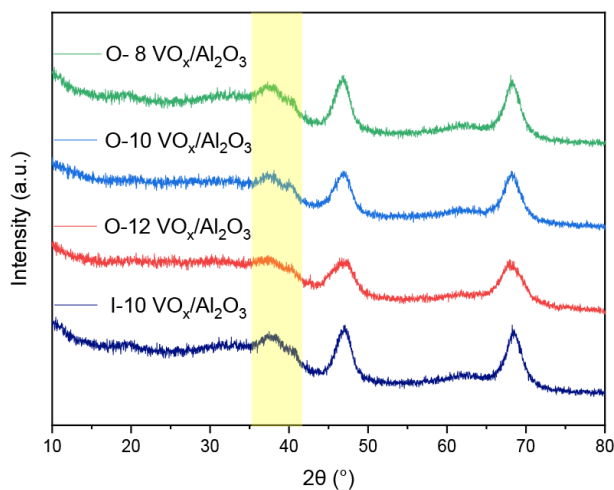


Figure 3. XRD patterns of the catalysts synthesized using the 1-pot method and I-10-VO_x/Al₂O₃ catalysts.

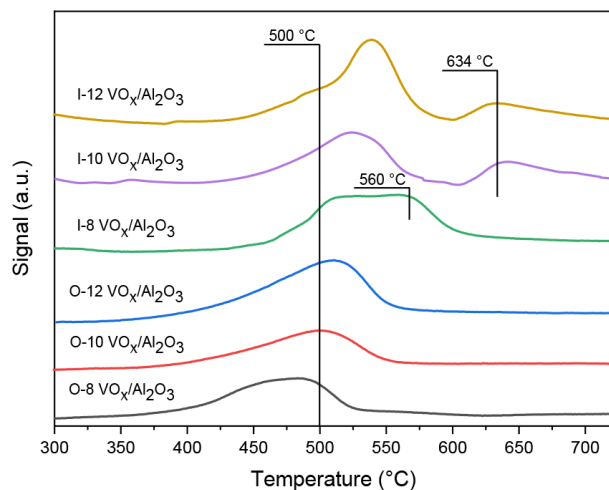


Figure 4. H₂-TPR profile of the catalysts.

represented the channel network and the dark areas represented the alumina matrix. Figure S1 shows the HRTEM image of the catalyst. No V₂O₅ crystallites were found, indicating that the vanadium species were mainly present as oligomers on the catalyst, which was consistent with the results of the XRD and H₂-TPR.

The element bonding configuration of the O-10-VO_x/Al₂O₃ catalysts was investigated by XPS to determine the electronic environment of the catalysts and the results also confirmed the existence of vanadium species. The XPS spectrum of the sample is shown in Figure 5c, where V, O, C, and Al were detected on the catalysts. The corresponding V 2p, O1s, and Al 2p of the XPS core-level spectra are shown in Figures 5d–5f. As can be seen in Figure 5d, V 2p_{3/2} and V 2p_{1/2} peaks were present in the V 2p spectrum due to the spin-orbit splitting of the P orbital. The deconvolution of V 2p_{3/2} presented 3 main components at 516.0 eV, 517.5 eV, and 518.9 eV, which can be assigned to V³⁺, V⁴⁺, and V⁵⁺, respectively [34,35]. The presence of V³⁺ and V⁴⁺ may have been responsible for the high catalytic activity and stability of the catalyst, since V³⁺ is the main active species and V⁴⁺ has better resistance to coke formation in a reaction [5,36]. The peak of O1s at 532 eV was related to the O-V bond, and the peak at 536 eV contributed to the C-O, C=O, and C-OH bonds [37]. Meanwhile, Figure 5f shows the high-resolution XPS spectrum of Al 2p. The peaks at 71.9 eV and 75.8 eV can be ascribed to the Al-O and Al-OH bonds, respectively [38]. Among them, the existence of a high proportion of Al-OH indicated that a large amount of hydroxyl groups were located on the surface of the catalyst, which was advantageous for increasing the catalytic activity of the catalyst [5]. Although the XPS spectrum showed the presence of vanadium, no obvious particles of vanadium oxide could be observed in the TEM image, indicating that vanadium oxide should be present at a size less than 1 nm or should form a solid solution with the support [39]. Thus, the vanadium species may have been anchored to the surface of the support in an oligomer state.

3.6. Reaction-regeneration cycles

In order to investigate the stability and reusability of the as-prepared catalysts, the O-10-VO_x/Al₂O₃ catalysts were tested via reaction-regeneration cycle experiments for PDH. The catalysts were regenerated in situ at 580 °C for 2 h in an air flow of 30 mL/min. After 4 h of PDH reaction, the flow was then switched to a N₂ flow of 30 mL/min for 1 h. As shown in Figure 6, the initial activity of the catalysts decreased over time in the

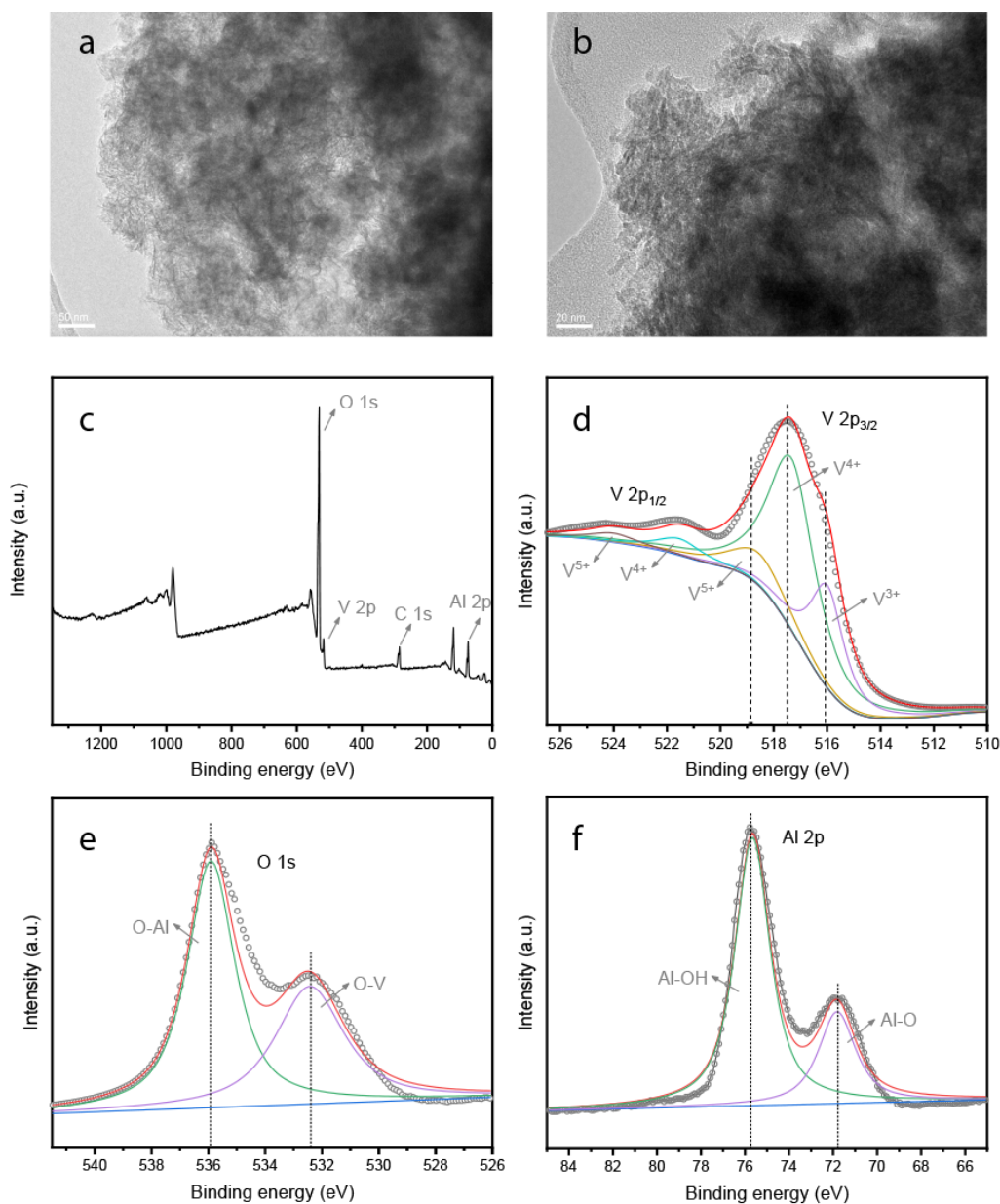


Figure 5. TEM images and XPS spectra of the as-prepared catalysts (a), TEM image of O-10-VO_x/Al₂O₃ (b), XPS spectra of O-10-VO_x/Al₂O₃ (c), V 2p (d), O 1s (e), and Al 2p core-level spectra (f).

first cycle due to deactivation of the catalysts caused by the formation of carbon. Subsequently, in the second cycle, it can be seen that the activity slightly decreased and the conversion of propane decreased slightly by about 5%, while selectivity of propylene increased by about 4%. The irreversible decrease of catalytic activity occurred in the second cycle, possibly because of the texture changes of the catalysts and the aggregation of the VO_x species [4]. After the first regeneration, the activity of the catalysts remained stable (propane conversion was between 43% and 48%, propylene selectivity was between 84% and 90%). This meant that the structure of the VO_x species and porous alumina had been stabilized.

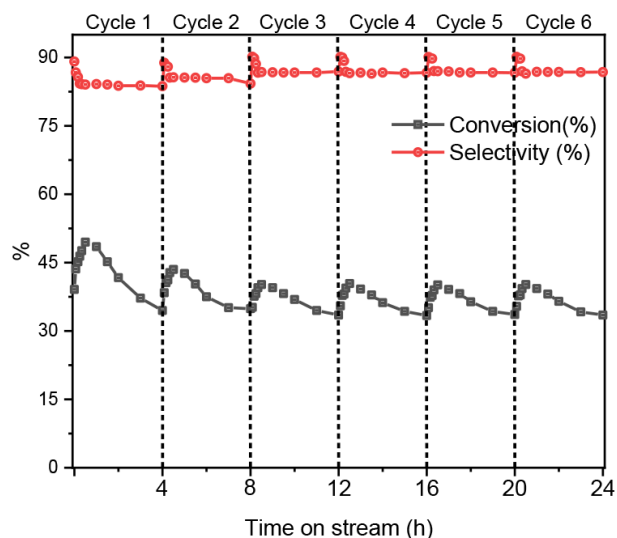


Figure 6. Propane conversion and propylene selectivity of reaction-regeneration cycles over the O-10-VO_x/Al₂O₃ catalyst.

3.7. Conclusions

The facile 1-pot synthesis of VO_x/Al₂O₃ catalysts with different vanadium contents for the significant enhancement of catalytic performance and stability for PDH was presented herein. These catalysts were highly efficient, cost-effective, and environmentally friendly, and vanadium is a low-polymerized VO_x species, which is the main active species for catalytic dehydrogenation. In addition, the O-10-VO_x/Al₂O₃ catalysts exhibited optimized catalytic performance. The obtained VO_x/Al₂O₃ catalysts had the following advantages: 1) Catalysts prepared by the 1-pot method had higher specific surface area and pore volume, which can increase the access between propane and the active sites. 2) The catalysts had higher catalytic performance than the VO_x/Al₂O₃ catalysts prepared by the IWI method. 3) The active sites were well dispersed and stable because the vanadium precursor and aluminum precursor were mixed in solution, and the introduction of CMC enhanced the interaction between the vanadium and aluminum during the assembly process.

Acknowledgments

The authors gratefully acknowledge the research grants provided by the Shandong Provincial Natural Science Foundation, China (ZR2018027, ZR2019BB052); the fund of the State Key Laboratory of Chemical Resource Engineering (Beijing University of Chemical Technology) (CRE-2018-C-3-2); and the Opening Project of Shandong Eco-chemical Engineering Collaborative Innovation Center (XTCXQN15).

References

1. Xiong C, Chen S, Yang P, Zha S, Zhao ZJ et al. Structure-performance relationships for propane dehydrogenation over aluminum supported vanadium oxide. *ACS Catalysis* 2019; 9 (7): 5816-5827. doi: 10.1021/acscatal.8b04701
2. Hu P, Lang WZ, Yan X, Chen XF, Guo YJ. Vanadium-doped porous silica materials with high catalytic activity and stability for propane dehydrogenation reaction. *Applied Catalysis A: General* 2018; 553: 65-73. doi: 10.1016/j.apcata.2018.01.014
3. Liu Q, Yang Z, Luo M, Zhao Z, Wang J et al. Vanadium-containing dendritic mesoporous silica nanoparticles: multifunctional catalysts for the oxidative and non-oxidative dehydrogenation of propane to propylene. *Microporous and Mesoporous Materials* 2019; 282: 133-145. doi: 10.1016/j.micromeso.2019.03.036

4. Yang QQ, Hu P, Xiu NY, Lang WZ, Guo YJ. $\text{VO}_x/\gamma\text{-Al}_2\text{O}_3$ catalysts for propane dehydrogenation prepared by “impregnation-solid phase reaction” method with aluminum hydroxide as support precursor. *ChemistrySelect* 2018; 3 (35): 10049-10055. doi: 10.1002/slct.201802070
5. Zhao ZJ, Wu T, Xiong C, Sun G, Mu R et al. Hydroxyl-mediated non-oxidative propane dehydrogenation over $\text{VO}_x/\gamma\text{-Al}_2\text{O}_3$ catalysts with improved stability. *Angewandte Chemie International Edition* 2018; 57 (23): 6791-6795. doi: 10.1002/anie.201800123
6. Liu G, Zeng L, Zhao ZJ, Tian H, Wu T et al. Platinum-modified $\text{ZnO}/\text{Al}_2\text{O}_3$ for propane dehydrogenation: minimized platinum usage and improved catalytic stability. *ACS Catalysis* 2016; 6 (4): 2158-2162. doi: 10.1021/acscatal.5b02878
7. Bakare IA, Adamu S, Qamaruddin M, Al-Bogami SA, Al-Ghamdi S et al. Oxidative dehydrogenation of propane to propylene over VO_x on mixed $\theta\text{-Al}_2\text{O}_3$ /alkaline earth metal oxides supports. *Industrial & Engineering Chemistry Research* 2019; 58 (25): 10785-10792. doi: 10.1021/acs.iecr.9b01144
8. Mitran G, Ahmed R, Iro E, Hajimirzaee S, Hodgson S et al. Propane oxidative dehydrogenation over VO_x /SBA-15 catalysts. *Catalysis Today* 2018; 306: 260-267. doi: 10.1016/j.cattod.2016.12.014
9. Barman S, Maity N, Bhatte K, Ould-Chikh S, Dachwald O et al. Single-site VO_x moieties generated on silica by surface organometallic chemistry: a way to enhance the catalytic activity in the oxidative dehydrogenation of propane. *ACS Catalysis* 2016; 6 (9): 5908-5921. doi: 10.1021/acscatal.6b01263
10. Ovsitser O, Schomaecker R, Kondratenko EV, Wolfram T, Trunschke A. Highly selective and stable propane dehydrogenation to propene over dispersed VO_x -species under oxygen-free and oxygen-lean conditions. *Catalysis Today* 2012; 192 (1): 16-19. doi: 10.1016/j.cattod.2012.01.034
11. Sokolov S, Stoyanova M, Rodemerck U, Linke D, Kondratenko EV. Comparative study of propane dehydrogenation over V-, Cr-, and Pt-based catalysts: Time on-stream behavior and origins of deactivation. *Journal of Catalysis* 2012; 293: 67-75. doi: 10.1016/j.jcat.2012.06.005
12. Bai P, Ma Z, Li T, Tian Y, Zhang Z et al. Relationship between surface chemistry and catalytic performance of mesoporous $\gamma\text{-Al}_2\text{O}_3$ supported VO_x catalyst in catalytic dehydrogenation of propane. *ACS Applied Materials & Interfaces* 2016; 8 (39): 25979-25990. doi: 10.1021/acsami.6b07779
13. Yang H, Lu Q, Gao F, Shi Q, Yan Y et al. One-step synthesis of highly ordered mesoporous silica monoliths with metal oxide nanocrystals in their channels. *Advanced Functional Materials* 2005; 15 (8): 1377-1384. doi: 10.1002/adfm.200500026
14. Sun Q, Wang N, Bing Q, Si R, Liu J et al. Subnanometric hybrid $\text{Pd-M}(\text{OH})_2$, $\text{M}=\text{Ni, Co}$, clusters in zeolites as highly efficient nanocatalysts for hydrogen generation. *Chem* 2017; 3 (3): 477-493. doi: 10.1016/j.chempr.2017.07.001
15. Liu L, Díaz U, Arenal R, Agostini G, Concepción P et al. Generation of subnanometric platinum with high stability during transformation of a 2D zeolite into 3D. *Nature Materials* 2017; 16 (1): 132. doi: 10.1038/nmat4757
16. Farmer JA, Campbell CT. Ceria maintains smaller metal catalyst particles by strong metal-support bonding. *Science* 2010; 329 (5994): 933-936. doi: 10.1126/science.1191778
17. Wang Y, Wang W, Xue F, Cheng Y, Liu K et al. One-pot synthesis of $\text{Pd}@ \text{Pt}_3\text{Ni}$ core-shell nanobranches with ultrathin $\text{Pt}_3\text{Ni}\{111\}$ skins for efficient ethanol electrooxidation. *Chemical Communications* 2018; 54 (41): 5185-5188. doi: 10.1039/C8CC02816H
18. Xia BY, Wu HB, Li N, Yan Y, Lou XW et al. One-pot synthesis of Pt-Co alloy nanowire assemblies with tunable composition and enhanced electrocatalytic properties. *Angewandte Chemie International Edition* 2015; 54 (12): 3797-3801. doi: 10.1002/anie.201411544

19. Hou C, Wang J, Du W, Wang J, Du Y et al. One-pot synthesized molybdenum dioxide-molybdenum carbide heterostructures coupled with 3D holey carbon nanosheets for highly efficient and ultrastable cycling lithium-ion storage. *Journal of Materials Chemistry A* 2019; 7 (22): 13460-13472. doi: 10.1039/C9TA03551F
20. Ji L, Yan P, Zhu C, Ma C, Wu W et al. One-pot synthesis of porous 1T-phase MoS₂ integrated with single-atom Cu doping for enhancing electrocatalytic hydrogen evolution reaction. *Applied Catalysis B: Environmental* 2019; 251: 87-93. doi: 10.1016/j.apcatb.2019.03.053
21. Hu P, Lang WZ, Yan X, Chu LF, Guo YJ. Influence of gelation and calcination temperature on the structure-performance of porous VO_x-SiO₂ solids in non-oxidative propane dehydrogenation. *Journal of Catalysis* 2018; 358: 108-117. doi: 10.1016/j.jcat.2017.12.004
22. Khalily MA, Eren H, Akbayrak S, Susapto HH, Biyikli N et al. Facile synthesis of three-dimensional Pt-TiO₂ nano-networks: a highly active catalyst for the hydrolytic dehydrogenation of ammonia-borane. *Angewandte Chemie International Edition* 2016; 55 (40): 12257-12261. doi: 10.1002/anie.201605577
23. Filez M, Redekop E, Poelman H, Galvita V, Meledina M et al. One-pot synthesis of Pt catalysts based on layered double hydroxides: an application in propane dehydrogenation. *Catalysis Science & Technology* 2016; 6 (6): 1863-1869. doi: 10.1039/C5CY01274K
24. Zhou X, Zou Y, Ma J, Cheng X, Li Y et al. Cementing mesoporous ZnO with silica for controllable and switchable gas sensing selectivity. *Chemistry of Materials* 2019; 31 (19): 8112-8120. doi: 10.1021/acs.chemmater.9b02844
25. Soler-Illia GDA, Louis A, Sanchez C. Synthesis and characterization of mesostructured titania-based materials through evaporation-induced self-assembly. *Chemistry of Materials* 2002; 14 (2): 750-759. doi: 10.1021/cm011217a
26. Brinker CJ, Lu Y, Sellinger A, Fan H. Evaporation-induced self-assembly: nanostructures made easy. *Advanced Materials* 1999; 11 (7): 579-585. doi: 10.1002/(SICI)1521-4095(199905)11:7<579::AID-ADMA579>3.0.CO;2-R
27. Zhu H, Anjum DH, Wang Q, Abou-Hamad E, Emsley L et al. Sn surface-enriched Pt-Sn bimetallic nanoparticles as a selective and stable catalyst for propane dehydrogenation. *Journal of Catalysis* 2014; 320: 52-62. doi: 10.1016/j.jcat.2014.09.013
28. Jang EJ, Lee J, Jeong HY, Kwak JH. Controlling the acid-base properties of alumina for stable PtSn-based propane dehydrogenation catalysts. *Applied Catalysis A: General* 2019; 572: 1-8. doi: 10.1016/j.apcata.2018.12.024
29. Sattler JJ, Mens AM, Weckhuysen BM. Real-time quantitative operando Raman spectroscopy of a CrO_x/Al₂O₃ propane dehydrogenation catalyst in a pilot-scale reactor. *ChemCatChem* 2014; 6 (11): 3139-3145. doi: 10.1002/cctc.201402649
30. Ma B, Li Y, Liu G, Liang D. Preparation and properties of Al₂O₃-MgAl₂O₄ ceramic foams. *Ceramics International* 2015; 41 (2): 3237-3244. doi: 10.1016/j.ceramint.2014.11.013
31. Bulushev DA, Rainone F, Kiwi-Minsker L, Renken A. Influence of potassium doping on the formation of vanadia species in V/Ti oxide catalysts. *Langmuir* 2001; 17 (17): 5276-5282. doi: 10.1021/la010077g
32. Berndt H, Martin A, Brückner A, Schreier E, Müller D et al. Structure and catalytic properties of VO_x/MCM materials for the partial oxidation of methane to formaldehyde. *Journal of Catalysis* 2000; 191 (2): 384-400. doi: 10.1006/jcat.1999.2786
33. Kondratenko E, Baerns M. Catalytic oxidative dehydrogenation of propane in the presence of O₂ and N₂O - The role of vanadia distribution and oxidant activation. *Applied Catalysis A: General* 2001; 222 (1-2): 133-143. doi: 10.1016/S0926-860X(01)00836-5
34. Fan K, Chen H, Ji Y, Huang H, Claesson PM et al. Nickel-vanadium monolayer double hydroxide for efficient electrochemical water oxidation. *Nature Communications* 2016; 7: 11981. doi: 10.1038/ncomms11981

35. Xing X, Liu R, Cao K, Kaiser U, Zhang G et al. Manganese vanadium oxide-N-doped reduced graphene oxide composites as oxygen reduction and oxygen evolution electrocatalysts. *ACS Applied Materials & Interfaces* 2018; 10 (51): 44511-44517. doi: 10.1021/acsami.8b16578
36. Xiong C, Chen S, Yang P, Zha S, Zhao ZJ et al. Structure-performance relationships for propane dehydrogenation over aluminum supported vanadium oxide. *ACS Catalysis* 2019; 9 (7): 5816-5827. doi: 10.1021/acscatal.8b04701
37. Ureña-Begara F, Crunteanu A, Raskin JP. Raman and XPS characterization of vanadium oxide thin films with temperature. *Applied Surface Science* 2017; 403: 717-727. doi: 10.1016/j.apsusc.2017.01.160
38. Iatsunskyi I, Kempinski M, Jancelewicz M, Załęski K, Jurga S et al. Structural and XPS characterization of ALD Al_2O_3 coated porous silicon. *Vacuum* 2015; 113: 52-58. doi: 10.1016/j.vacuum.2014.12.015
39. Kondratenko EV, Cherian M, Baerns M, Su D, Schlögl R et al. Oxidative dehydrogenation of propane over V/MCM-41 catalysts: Comparison of O_2 and N_2O as oxidants. *Journal of Catalysis* 2005; 234 (1): 131-142. doi: 10.1016/j.jcat.2005.05.025

Supplemental information

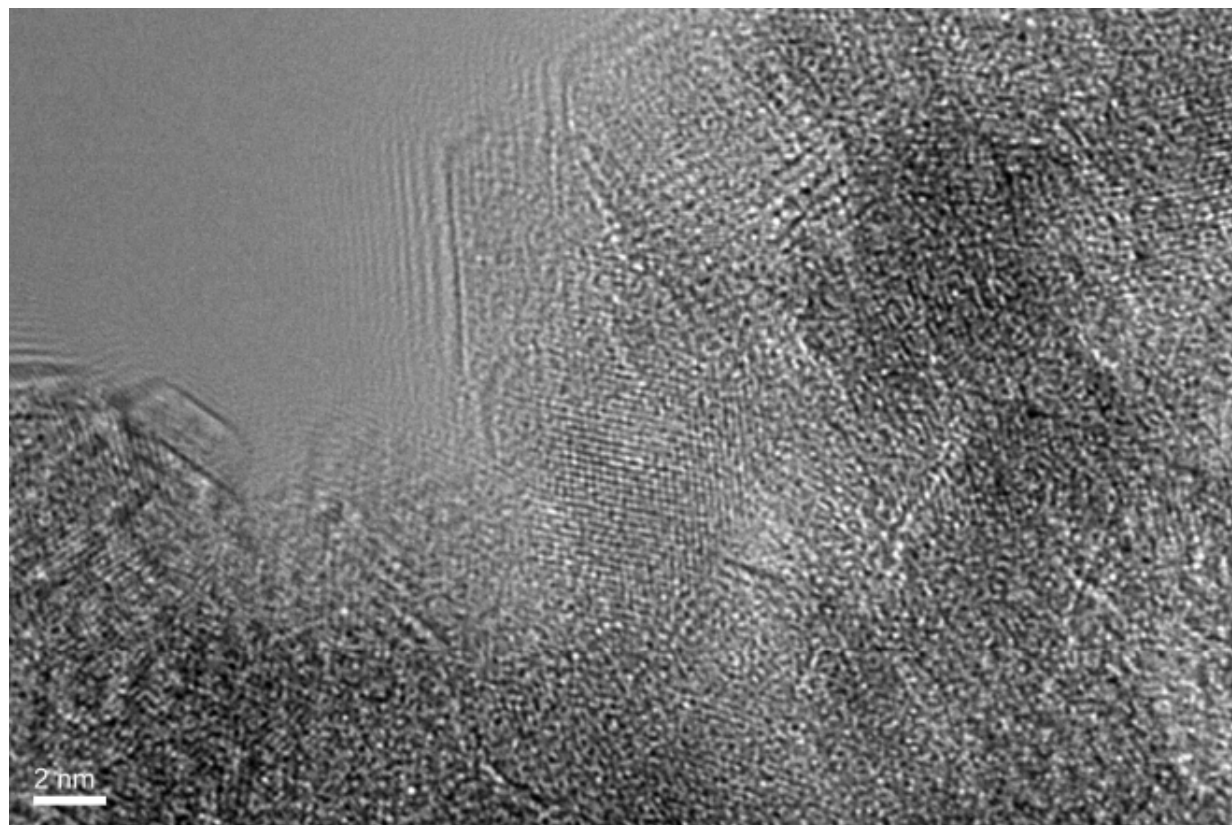


Figure S1. High-magnification TEM image of O-10-VO_x/Al₂O₃.

Table S1. TOF value and propylene selectivity over the vanadium-based catalysts in PDH.

| Catalysts | V (wt.%) | TOF ×10 ⁻³ (s ⁻¹) | Propylene selectivity (%) |
|------------------------------------------------------|----------|--------------------------------------------------|---------------------------|
| O-8-VO _x /Al ₂ O ₃ | 8 | 2.7 (1 h ^a); 1.7 (4 h ^b) | ~ 85 |
| O-10-VO _x /Al ₂ O ₃ | 10 | 3.1 (1 h); 2.1 (4 h) | ~ 84 |
| O-12-VO _x /Al ₂ O ₃ | 12 | 2.1 (1 h); 1.6 (4 h) | ~ 80 |
| I-8-VO _x /Al ₂ O ₃ | 8 | 2.9 (1 h); 2.0 (4 h) | ~ 81 |
| I-10-VO _x /Al ₂ O ₃ | 10 | 2.8 (1 h); 1.8 (4 h) | ~ 81 |
| I-12-VO _x /Al ₂ O ₃ | 12 | 2.2 (1 h); 1.4 (4 h) | ~ 77 |

^a Initial 1 h of reaction, ^b Initial 4 h of reaction.